Available online at www.sciencedirect.com
SCIENCE DIRECT
Carbohydrate Polymers 60 (2005) 379–389
Carbohydrate Polymers
www.elsevier.com/locate/carbpol

Enzyme and acid resistance of amylose-lipid complexes differing in amylose chain length, lipid and complexation temperature

Greta G. Gelders*, Jeroen P. Duyck, Hans Goesaert, Jan A. Delcour

Laboratory of Food Chemistry, Department of Food and Microbial Technology, Katholieke Universiteit Leuven, Kasteelpark Arenberg 20, B-3001 Leuven, Belgium

Received 13 August 2004; accepted 2 February 2005
Available online 7 April 2005

Abstract

To study parameters that influence enzyme and acid resistance of amylose-lipid complexes, complexes were formed between amylose of different average chain lengths [Degree of Polymerisation (DP); DP60, 400, 950] and docosanoic acid (C22) or glyceryl monostearate (GMS) at 60 or 90 °C. Complexes were hydrolysed with hog pancreatic alpha-amylase or acid (2.2 N HCl). DP400- and DP950-complexes were of type I when formed at 60 °C and of type II when formed at 90 °C. Enzyme and acid resistance increased with increasing amylose DP, lipid chain length and complexation temperature. DP60 yielded only type I complexes, independent of the complexation temperature. Enzymic and acid hydrolysis of all complexes gave rise to two or more dextrin subpopulations, which are interpreted to originate from a sequence of lamellar units (the smallest peak DP) with interconnecting, amorphous amylose chains. The peak DP of such lamellar unit increased with increasing amylose DP and complexation temperature, but remained constant when higher enzyme dosages were applied. Synthesis of amylose-lipid complexes from amylose and lipids of variable structure under variable temperature conditions followed by hydrolysis can yield dextrin populations of defined and relatively narrow molecular weight distributions.

Keywords: Complexation; V-amylose; Enzymic and acid hydrolysis; Chain length

1. Introduction

Since its discovery by de Claubry, 1953 the blue starch-iodine complex has been extensively studied. Amylose forms a left-handed helix with 6 glucose moieties (7 or 8 for more bulky guest molecules) per helix turn with an inner diameter of ~0.5 nm and a pitch height of ~0.805 nm not only with iodine, but also with lipids, alcohols, dimethylsulfoxide, etc. When complexed at temperatures of at least 90 °C, single amylose-lipid helices are packed into a crystalline orthorombic unit cell, resulting in the characteristic V-type wide angle X-ray diffraction (WAXD) pattern for type II_a and II_b complexes. At complexation temperatures of maximally 60 °C, amylose-lipid helices are not organised in a crystalline packing and result in so-called type I complexes with low-temperature (<100 °C) melting endotherms and amorphous X-ray diagrams (Biliaderis & Galloway, 1989; Buléon, Colonna, Planchot, & Ball, 1998; Godet, Bizot, & Buléon, 1995).

Enzyme and acid resistance of amylose-lipid complexes has been less studied. Holm, Björck, Ostrowska, Eliasson, Asp, Lundquist, Larsson (1983) examined in vitro and in vivo digestibilities of amylose-lipid complexes and concluded that complexed amylose is hydrolysed and absorbed in the gastrointestinal tract to the same extent as free amylose but somewhat slower. Eliasson and Krog (1985) and Jane and Robyt (1984) compared the enzyme resistance of several amylose-alcohol and amylose-monoacylglycerol complexes, respectively. All these studies dealt with type I complexes. At that time, one was not aware of the existence of two thermally and morphologically distinct complex types (I and II), such as shown later by Biliaderis and Galloway (1989) based on the work of Kowblansky (1985). In the following years, enzymic and acid hydrolysis were applied to investigate structural differences between type I, II_a and II_b complexes and to determine the length of the ordered regions in the complexes (Biliaderis & Galloway, 1989; Biliaderis & Seneviratne, 1990; Galloway, Biliaderis,

* Corresponding author. Tel.: +32 16 32 16 34; fax: +32 16 32 19 97.
E-mail address: greet.gelders@biw.kuleuven.be (G.G. Gelders).

0144-8617/$ - see front matter © 2005 Elsevier Ltd. All rights reserved.
doi:10.1016/j.carbpol.2005.02.008

& Stanley, 1989; Seneviratne & Biliaderis, 1991). The main findings were that the rate and extent of degradation of the complexes decreased in the order type I > type II_a > type II_b and was therefore, inversely related to the degree of organisation in the complexes (Seneviratne & Biliaderis, 1991). Resistant amylodextrins of type II complexes had a larger degree of polymerisation (DP) than those of type I complexes. Galloway et al. (1989) ascribed this to super-cooling effects, resulting in thicker lamellae for type II complexes. The above-mentioned studies focused on the impact of the nature of lipids and complexation temperature on the enzyme or acid resistance of amylose-lipid complexes. Amylose DP (1150) was constant. Godet, Bouchet, Colonna, Gallant, and Buléon (1996) formed complexes at 90 °C, promoting type II complexes, with different amylose populations (DP30, 40, 80 and 900) and three fatty acids (C8, C12 and C16). After *Bacillus subtilis* alpha-amylase hydrolysis of these highly crystalline amylose-fatty acid complexes, they found that crystal thickness depends strongly on amylose chain length and to a lesser extent on fatty acid chain length.

In this study, we evaluated parameters (lipid, amylose chain length, complexation temperature) affecting enzyme and acid resistance of amylose-lipid complexes. To this end, amyloses of different DP (DP60, DP400, DP950) were complexed with glyceryl monostearate (GMS) and docosanoic acid (C22) at 60 and at 90 °C. The obtained complexes were hydrolysed with hog pancreatic alpha-amylase (HPA) or acid (2.2 N HCl) and the residues were analysed with WAXD, differential scanning calorimetry (DSC), high performance anion-exchange chromatography (pulsed amperometric detection, HPAEC-PAD), and high performance size exclusion chromatography (refractive index detection, SEC) to examine the chain length distribution of the resistant residues. In doing so, we aimed to obtain new structural insights in amylose-lipid complexes by linking our results with those of previous work by Godet et al. (1996) and Seneviratne and Biliaderis (1991).

2. Experimental

2.1. Materials

Three amylose fractions, with peak DP 60, 400 and 950, were prepared from starch sources as described in Gelders, Vanderstukken, Goesaert, and Delcour (2004). All amylose fractions were defatted with 85% methanol for 24 h in a Soxhlet extractor prior to complexation.

Lipids used were docosanoic acid (C22), purchased from Acros Organics (Geel, Belgium), and Dimodan PVP (glyceryl monostearate, GMS) (purity > 90%), kindly donated by Danisco (Brabrand, Denmark). Hog pancreatic alpha-amylase (HPA) [EC3.2.1.1] was from Fluka (Fluka 10080; Steinheim, Germany). All other reagents were of at least analytical grade and supplied by Sigma-Aldrich (Bornem, Belgium).

2.2. Methods

2.2.1. Amylose-lipid complexation

Each amylose fraction (4.0 g) was dissolved in 25.0 ml hot DMSO and diluted with 375 ml boiling water. The resulting solutions (1.0% w/v) were boiled (30 min) and equilibrated in a water bath at 60 or 90 °C. C22 or GMS (0.8 g), dissolved in 20.0 ml hot 95% ethanol, was then slowly added under vigorous mixing. Complexes were isothermally grown for 240 min with gentle stirring every 30 min. Mixtures were slowly cooled (12 h) to ambient temperature and recovered by centrifugation (10,000 *g*, 30 min, 6 °C). The recovered complexes were washed (200 ml water), centrifuged (10,000 *g*, 15 min, 6 °C), suspended, frozen with liquid nitrogen and freeze-dried. The gently powdered (250 μm) complexes were washed (30 min) in chloroform (60 ml/g complex) at ambient temperature to remove excess free lipids. The complex suspensions were filtered over a crucible with a sintered glass filter (porosity 4) and thoroughly washed with chloroform. The chloroform washed complexes were air dried. The 12 complexes obtained are labelled with the following information-bearing codes 'DP of amylose fraction-lipid-complexation temperature' (e.g. DP950-GMS-60 °C).

2.2.2. Hydrolysis of amylose-lipid complexes

2.2.2.1. Enzymic hydrolysis. HPA was extracted from the Fluka preparation (137 mg) with 200 ml water containing 5 mM $CaCl_2$ and 0.5 g/l BSA (pH 6.9, solution A). One Unit (U) of HPA activity was defined as the amount of enzyme needed to yield an increase in extinction (590 nm) of 1.0 at pH 6.9 in the Amylazyme® method, described in the Megazyme data sheet AMZ 8/96 (Bray, Ireland). All complexes (250 mg) were suspended in 29 ml solution A and equilibrated in a water bath at 30 °C. 1.0 ml of a five times diluted HPA extract (~20 U) was added to the suspension under continuous stirring (250 rpm). DP400-GMS-60 °C and DP400-GMS-90 °C were additionally hydrolysed by 40 U (2.5 times diluted HPA extract) and 100 U (undiluted HPA extract) HPA, respectively.

At selected time intervals, aliquots (0.5 ml) were removed from the suspensions and immediately analysed as described in Section 2.2.2.3.

After 24 h, the mixture was centrifuged (10,000*g*, 30 min, 6 °C). The residue was washed (15 min) with 50 ml 1.0 M NaCl at 6 °C to remove adsorbed HPA (Kitahara, Suganuma, & Nagahama, 1996), and centrifuged (10,000*g*, 15 min, 6 °C). A final washing step (15 min at 6 °C) with 50 ml water was performed to remove salt, and followed by centrifugation (10,000*g*, 15 min, 6 °C).

The residues were frozen with liquid nitrogen and then freeze-dried.

2.2.2.2. Acid hydrolysis. DP400-GMS-60 °C and DP400-GMS-90 °C complexes (250 mg) were suspended in 50 ml 2.2 N HCl at 30 °C. Complex suspensions were shaken twice a day by hand. Hydrolysis was terminated after 7 days by centrifugation (10,000*g*, 30 min, 6 °C). Residues were suspended in water (50 ml), neutralised with 0.5 M NaOH (pH 7.0) and centrifuged (10,000*g*, 15 min, 6 °C). A final washing step (15 min) with 50 ml water was performed to remove formed salt. Following centrifugation (10,000*g*, 15 min, 6 °C), the complex residues were frozen with liquid nitrogen and freeze-dried.

2.2.2.3. Degree of hydrolysis in function of time. Aliquots of the complex suspensions were centrifuged (10,000*g*, 5 min) and the total glucose content in the supernatant was determined in triplicate by the phenol-sulphuric acid method (Dubois, Gilles, Hamilton, Rebers, & Smith, 1956). Degree of hydrolysis (DH) was determined by expressing the total glucose content (in the supernatant) as a percentage of the total glucose content [determined by gas chromatography (Englyst & Cummings, 1984)] of the initial complex. DH values were fitted using the Levenberg–Marquardt non-linear least-squares curve fitting algorithm with the following equation:

$$y = A_1(1 - \exp^{-x/t_1}) + A_2(1 - \exp^{-x/t_2}) \quad (1)$$

with y, the degree of hydrolysis, DH (%) and x, the hydrolysis time (h). The first term, with constants A_1 and t_1, concerns the easily degradable fraction (first part of the hydrolysis curve). A_2 and t_2 are constants representing the slowly degradable, crystalline fraction (second part of the hydrolysis curve). R^2 was at least 0.99 for al fitted curves. Several parameters were derived from the fitted curves to aid the interpretation of the observed hydrolysis data. The initial and final hydolysis rates V_i and V_f were calculated as the slope at $x = 0.5$ h and $x = 23.5$ h, respectively, as the first derivative of Eq. (1) [see Eq. (2)]. A_1 was defined as the easily degradable fraction (EDF). The final DH (FDH) was that after 24 h (enzymic hydrolysis) or after 7 days (acid hydrolysis).

$$\frac{dy}{dx} = \frac{A_1}{t_1}\exp^{(-x/t_1)} + \frac{A_2}{t_2}\exp^{(-x/t_2)} \quad (2)$$

2.2.3. X-ray diffraction and determination of relative crystallinity

WAXD measurements were performed with Ni-filtered Cu K_α radiation on a Rigaku rotating anode device (Manners, USA) operating at 40 kV and 100 mA, using a Rigaku high temperature X-ray diffractometer (Manners, USA). Detection was with a scintillation counter with a powder diffractometer operated in transmittance. Samples (moisture content ca. 5%) were sealed between two pieces of aluminum tin foil. The scanning rate was 10 s per step of 0.05° 2θ (with 2θ the diffraction angle) over a range of 3–33° 2θ. Amorphous waxy maize starch was prepared in a rotating flask by heating an aqueous starch suspension (2.0% w/v) at 85 °C for 20 min. The dilute paste was then boiled (100 °C) for 1 h. The sample was frozen with liquid nitrogen and freeze-dried. Diffraction patterns of amylose-lipid complex residues and the amorphous sample were normalised to the total diffused intensity between 6 and 30° 2θ. The normalised amorphous diffraction pattern was fitted to the main minima of the normalised amylose-lipid complex diffraction pattern. The relative crystallinity (X_c) between 6 and 30° 2θ was calculated using the formula:

$$X_c = \frac{(S_{sample} - S_{amorphous})}{S_{sample}} \quad (3)$$

with S_{sample} integrated intensity of normalised amylose-lipid complex residue diffraction pattern; $S_{amorphous}$ integrated intensity corresponding to the fitted amorphous sample.

2.2.4. Differential scanning calorimetry

DSC was performed with a Seiko DSC 120 (Kawasaki Kanagawa, Japan). Samples (2–4 mg) were accurately weighed into coated aluminum sample pans and water was added (1:3 w/w sample dm/water). The pans were sealed, weighed and equilibrated overnight at room temperature to distribute the water evenly in the sample. After checking pan weight for possible moisture loss, the sample pan and an empty reference pan were heated from 30 °C to 135 °C at 4 °C/min. Calibration was with indium and tin. Onset (T_o), peak (T_m), conclusion (T_c) (dissociation) temperatures and enthalpies (ΔH) of amylose-lipid complex residues were determined with Seiko software. ΔH was expressed as J/g complex residue dry matter and temperatures in degree celsius. Results were averages of at least triplicate measurements. The coefficient of variation, defined as the ratio of the standard deviation and the mean of the obtained results was less than 3.0% for T_m. For ΔH values, respective standard deviations are given.

2.2.5. High performance size-exclusion chromatography

The (peak) DP values of the amylose-lipid complex residues were determined with SEC on a Superose 12TM column (fractionation range 1×10^3–3×10^5 M_r globular proteins; 30 cm × 1 cm) (Amersham Biosciences, Uppsala, Sweden). Calibration was with Shodex P-82 pullulan standards (Showa Denko, Japan), maltoheptaose and glucose (Sigma-Aldrich, Bornem, Belgium). Roger, Axelos, and Colonna (2000) reported that pullulans can be used to replace linear amylose standards for chromatographic calibration purposes when 0.1 M potassium hydroxide is used as eluent. A second order polynomial correlation was found between the logarithm (M_r standards) and the elution

volume. Each eluted peak was characterised by the peak DP (=M_r/162). It is this DP value which is used in the present paper.

A Biologic Duo Flow Core System (Bio-Rad Laboratories, Hercules, CA, USA) equipped with a Signal Import Module-HR (SIM-HR) and a RID-10A Detector (Shimadzu, Kyoto, Japan) was used. Samples (15 mg) were solubilised for at least 12 h in 1.0 M potassium hydroxide under mild magnetic stirring and then diluted with 9 volumes of water. After filtration (0.45 μm; regenerated cellulose syringe filter), 100 μl of the solubilised samples were injected. Elution was with 0.1 M potassium hydroxide (containing 0.02% sodium azide) at a flow rate of 0.5 ml/min and at ambient temperature.

2.2.6. High-performance anion-exchange chromatography with pulsed amperometric detection

HPAEC-PAD was performed with a Dionex DX-500 chromatography system (Sunnyvale, CA, USA). Sample preparation was as described in Section 2.2.5. The filtered (0.45 μm; regenerated cellulose syringe filters) samples were injected (25 μl) onto a CarboPac PA-100 anion-exchange column (250×4 mm) in combination with a CarboPac PA-100 guard column. The pulse potentials and durations, the eluents and the eluent gradient programme were as described by Gelders, Bijnens, Loosveld, Vidts, and Delcour (2003).

3. Results and discussion

3.1. Degree of hydrolysis of amylose-lipid complexes in function of time

Fig. 1 represents hydrolysis curves for all complexes hydrolysed with 20 U HPA. Two stage hydrolysis kinetics are observed with a first rapid stage during which amorphous parts and crystal defects are hydrolysed, and a second, slower stage in which the crystalline amylose-lipid helices are degraded (Godet et al., 1996; Seneviratne & Biliaderis, 1991). The first stage is characterised by high hydrolysis rates (V_i), the second stage, ideally reaching a plateau, by very low hydrolysis rates (V_f). The highest DH was obtained for the DP60-complexes, irrespective of the complexation temperature. A decreasing trend in DH was observed with increasing amylose chain length and complexation temperature. The difference in DH between complexes formed at 60 or at 90 °C increased with increasing amylose DP.

Several hydrolysis parameters (defined as in Section 2.2.2.3) were determined by means of the fitted curve (Eq. (1)) to observe differences in enzyme or acid resistance of the amylose-lipid complexes (Table 1). To distinguish the two hydrolysis stages, hydrolysis curves are often plotted in a semi-logarithmic form [log (100/100-DH)] as a function of time (Robin, Mercier, Charbonnière, & Guilbot, 1974). By extrapolation of the second stage to $x=0$ h, the EDF is estimated, as Robin, Mercier, Duprat, Charbonnière, and Guilbot (1975) introduced. However, the extrapolation of V_f to time zero is sometimes done without a semi-logarithmic conversion (Godet et al., 1996). In our opinion, this is only justified for small FDH, otherwise EDF is overestimated. For this reason, it is not applicable to our rather high FDH values. In addition, as only a small number of data points in the first hours of hydrolysis is available, the Robin procedure for determining V_i would involve a too low number of data points (at $x=0$ and 1 h). We therefore, fitted our data with a two-term function, one representing the hydrolysis of amorphous parts and the other the hydrolysis of crystalline helices. We defined EDF as the constant A_1.

Table 1 shows V_i, V_f, FDH and EDF values for 20 U HPA residues and will be discussed in that order. The higher

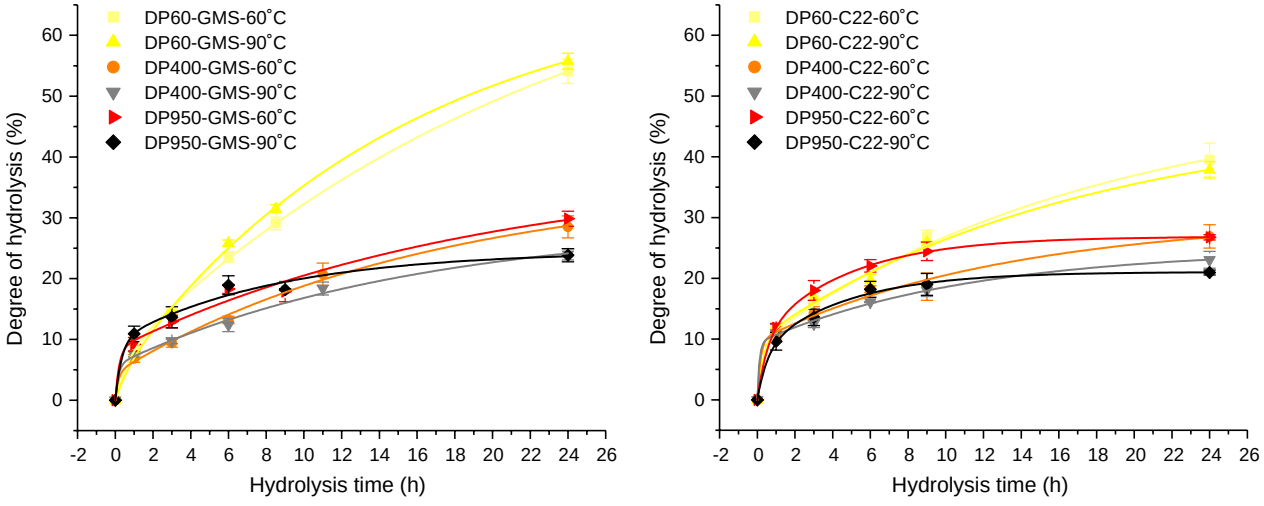

Fig. 1. Degrees of hydrolysis versus time for amylose (DP60, DP400 and DP950) complexed with glyceryl monostearate (GMS) or docosanoic acid (C22) at 60 or 90 °C and hydrolysed with 20 U hog pancreatic alpha-amylase (HPA).

Table 1
Hydrolysis of amylose-lipid complexes-differing in DP (DP60, DP400 and DP950), lipid type (GMS and C22) and complexation temperature (60 and 90 °C)-by 20, 40 or 100 U hog pancreatic alpha-amylase (HPA) or acid (2.2 N HCl). Hydrolysis characteristics, V_i, V_f, EDF, determined from hydrolyis degree curves as a function of time (Fig. 1)

Complex (20 U HPA)[a]	V_i (%/h)[b]	V_f (%/h)[c]	FDH (%)[d]	EDF (%)[e]	Crystallinity (%) (100−EDF)	Relative crystallinity (%)[f]
DP60 - GMS - 60 °C	7.65	1.17	54.1	74.5	25.5	71.4
DP60 - GMS - 90 °C	6.69	0.92	55.8	65.7	34.3	72.2
DP60 - C22 - 60 °C	8.58	0.62	39.5	41.1	58.9	71.3
DP60 - C22 - 90 °C	8.76	0.54	37.9	36.8	63.2	73.2
DP400 - GMS - 60 °C	3.12	0.46	28.5	31.7	68.3	75.9
DP400 - GMS - 90 °C	3.03	0.34	24.0	23.5	76.5	82.7
DP400 - C22 - 60 °C	4.15	0.26	26.9	20.3	79.7	78.9
DP400 - C22 - 90 °C	2.19	0.17	23.1	15.5	84.5	77.3
DP950 - GMS - 60 °C	4.95	0.46	29.8	29.8	70.2	72.3
DP950 - GMS - 90 °C	8.16	0.11	23.8	14.8	85.2	82.7
DP950 - C22 - 60 °C	10.67	0.03	26.7	16.6	83.4	68.6
DP950 - C22 - 90 °C	8.42	0.02	21.0	13.1	86.9	74.7
DP400 - GMS - 60 °C 40 U HPA	6.34	0.62	33.9	39.5	60.5	75.9
DP400 - GMS - 90 °C 100 U HPA	11.25	0.52	40.7	36.4	63.6	82.7
DP400 - GMS - 60 °C acid	1.11	0.11	57.8	53.8	46.3	75.9
DP400 - GMS - 90 °C acid	1.72	0.04	21.3	21.5	78.5	82.7

[a] Unless other hydrolysis conditions specified.
[b] V_i initial hydrolysis rate, determined as the slope in $x=0.5$ h.
[c] V_f final hydrolysis rate, determined as the slope in $x=23.5$ h (HPA hydrolysis) or in $x=167.5$ h (acid hydrolysis).
[d] FDH final degree of hydrolysis at 24 h (HPA hydrolysis) or at 7 days (acid hydrolysis).
[e] EDF easily degradable fraction, corresponding to constant A_1 (see Eq. (1)).
[f] Relative crystallinity of original amylose-lipid complexes determined with Wide Angle X-ray Diffraction (Gelders et al., 2004).

enzyme dosages and acid hydrolysis will be evaluated at the end of this section. Section 3.2 deals with the crystallinity data, presented in Table 1.

Table 1 reveals that V_i is the lowest for DP400-complexes and that it is higher for complexes formed at 60 °C except for the DP950-GMS-complexes. That this trend is not so well defined for the DP60-complexes is another indication for our hypothesis that only one type of complex exists for such short amylose chain lengths (Gelders et al., 2004). V_i is in most cases larger for C22-complexes than for corresponding GMS-complexes. This is in agreement with Godet et al. (1996) who reported for large amylose DPs a V_i increase with increasing fatty acid chain length.

V_f decreases with amylose DP and is higher for 60 °C-complexes than for their 90 °C-counterparts. V_f is almost twice as high for GMS-complexes than for the corresponding C22-complexes.

FDH and EDF decrease with increasing amylose DP and are markedly lower for the DP400- and DP950-complexes, formed at 90 °C, than for the 60 °C-complexes. The apparent contradictory higher EDF than FDH value for DP60-GMS-complexes can be explained when assuming that not all the easily degradable material is hydrolysed after 24 h. The hydrolysis curves of these complexes (Fig. 1) still show increases rather than reaching a plateau. This influences the A_1 and A_2 values, and thus EDF. FDH and EDF are larger for GMS-complexes than for the corresponding C22-complexes. This somewhat conflicts with Godet et al. (1996) who reported a FDH decrease for decreasing amylose DP and an EDF and an FDH increase for increasing fatty acid chain length. Eliasson and Krog (1985), however, reported that complexes with long saturated monoacylglycerols are more resistant to enzymic breakdown than complexes with shorter or more unsaturated monoacylglycerols.

In our view, the hydrolysis data obtained with our experimental setup can be explained on the basis of a longer amylose helix or higher lamellae thickness for C22 complexes (Gelders et al., 2004). The amylose DP determines the amount of helices that can be formed, which, in our opinion, is larger for the highest amylose DPs, resulting in less easily degradable amylose. Therefore, the lowest FDH and EDF is obtained for complexes formed with DP950 and C22 at 90 °C. We are aware that we compare two different lipid types and that the compactness of GMS-complexes is possibly lower than that of C22-complexes due to the bulky hydrophilic glycerol group and hence longer interconnecting amylose parts between lamellae.

When higher HPA dosages are added to the DP400-GMS-complexes, FDH increases. Also V_i and V_f increase compared to the corresponding 20 U HPA complex residues, as does the EDF. Acid hydrolysis of DP400-GMS-complexes occurs much slower than HPA hydrolysis. After 24 h acid hydrolysis of DP400-GMS-60 °C and DP400-GMS-90 °C, a DH of 19.2% and a DH of 7.5% was reached, respectively (results not shown). V_i and V_f

are subsequently much smaller than rates obtained in HPA hydrolysis. FDH and EDF (after 7 days) are much higher for the DP400-GMS-60 °C complex and indicate a structural difference between the DP400-GMS complex formed at 60 or at 90 °C. HPA and acid hydrolysis experiments confirm that high amylose DP complexes formed at 60 °C, resulting in type I complexes, are less acid and enzyme resistant than their counterparts formed at 90 °C. For shorter amylose (DP60) complexes, enzyme, and probably acid resistance as well, remains the same as we believe that only one type of complex exists.

3.2. Relative crystallinity of hydrolysis residues

Relative crystallinities of the different amylose-lipid complexes (Table 1), determined with WAXD, increased for increasing amylose DP (DP60 and DP400) due to improved crystalline features and crystallite size (Gelders et al., 2004). The slightly lower relative crystallinity for the DP950-complexes can be attributed to conformational disorders, which are more likely to occur for the longest amylose (DP950) and result in crystal defects (Godet, Tran, Colonna, Buléon, & Pezolet, 1995). Only for DP400- and DP950-complexes, the difference in relative crystallinity between complexes formed at 60 or 90 °C was substantial. We are aware that complexes formed at 60 °C result in a semi-crystalline V-pattern, contrary to most literature. Biliaderis and Seneviratne (1990) explained this to be the result of the drying procedure applied to the complexes. Freeze-drying, as was also here the case, modifies the structure of type I complexes by formation of chain aggregates of a much higher order.

Crystallinity values can also be deduced from EDF values (=100−EDF). The estimated crystallinity values (100−EDF) are of the same order of magnitude as the relative crystallinities determined by WAXD, except for the DP60-complexes, and increase with increasing amylose DP. However, the A_1 and A_2 values are affected by the fact that hydrolysis curves of the DP60-complexes are not levelling off.

After hydrolysis with 20 U HPA (Table 2), residues preserved their V-patterns and diffraction peaks became even sharper, indicating crystal enrichment and/or perfection. Literature data are, however, less clear. On the one hand, a decrease in crystallinity after enzymic treatment has been reported and even a polymorphic transition from V to B-type has been observed (Godet et al., 1996). On the other hand, Seneviratne and Biliaderis (1991) described that crystallinity before and after amylolysis does not change, except for some diffraction peak broadening. The latter was concluded by visual interpretation of V-patterns.

We believe that the present hydrolysis conditions are not as severe as in the mentioned studies and assume that mainly amorphous material was hydrolysed. The relative proportion of crystals therefore, is more important. Moreover, we do not exclude reorganisation of resistant amylose-lipid helices during freeze-drying of the residue. This explains the higher relative crystallinities after hydrolysis. Higher dosages of HPA and acid hydrolysis of DP400-GMS-60 °C and DP400-GMS-90 °C do yield residues with a reduced relative crystallinity (Table 2).

3.3. Thermal stability of hydrolysis residues

Table 3 presents thermal properties of the residual complexes. They follow the same trend as the original complexes (Gelders et al., 2004). T_m increases with increasing amylose DP (DP60 and DP400) due to improved crystalline features and larger crystallite size. DP950-complexes, however, have a similar or slightly lower T_m than the DP400-complexes, which can be explained by crystal defects resulting in a lower relative crystallinity (Table 1). DP60 amylose yielded, irrespective of the complexation temperature, predominantly type I complexes and this is still the case for its residues. Complex residues with DP400 and DP950 amylose are rather of type II when formed at 90 °C than when formed at 60 °C. T_m remains higher for C22-complex residues than for those of GMS-complexes as we expect a larger helical chain length for the former complexes. The total $\Delta H_{residue}$ (sum of ΔH where

Table 2
Relative crystallinity (%) of amylose-lipid complexes obtained with amylose (DP60, 400 and 950) complexed with glyceryl monostearate (GMS) or docosanoic acid (C22) at 60 or 90 °C, after enzymic (hog pancreatic alpha-amylase; HPA) or acid (2.2 N HCl) hydrolysis

Amylose	Hydrolysis	GMS		C22	
		60 °C	90 °C	60 °C	90 °C
DP60	20 U HPA	78.5	86.0	81.1	84.8
DP400	20 U HPA	85.8	94.0	92.8	96.9
	40 U HPA/100 U HPA[a]	81.0	81.2	–	–
	Acid	78.4	76.9	–	–
DP950	20 U HPA	80.0	84.0	77.2	85.2

[a] DP400-GMS-60 °C and DP400-GMS-90 °C complexes were hydrolysed with 40 and 100 U HPA, respectively.

Table 3
Dissociation temperatures, T_m (°C) and enthalpies, ΔH (J/g dm complex residue) of complexes produced from amylose (DP60, 400 or 950) and glyceryl monostearate (GMS) or docosanoic acid (C22) at 60 or at 90 °C and hydrolysed by hog pancreatic alpha-amylase (HPA) or acid (2.2 N HCl)

Amylose	Hydrolysis		GMS					C22			
			60 °C		90 °C			60 °C		90 °C	
			T_m(°C)	ΔH (J/g dm)	T_m(°C)	ΔH (J/g dm)		T_m(°C)	ΔH (J/g dm)	T_m(°C)	ΔH (J/g dm)
DP60	*20 U HPA*	FL	53.13	8.70 (0.35)	53.15	8.67 (0.06)	FL	74.78	1.25 (0.19)	73.70	0.57 (0.46)
		I	91.93	20.77 (2.40)	93.87	19.50 (3.47)	I	96.60	20.98 (1.24)	92.97	24.63 (2.17)
		II	–	–	112.55	3.60 (0.57)	II	–	–	105.40	
DP400	*20 U HPA*	FL	53.15	2.10 (0.26)	53.15	2.13 (0.32)	FL	–	–	–	–
		I	97.63	31.73 (4.36)	–	–	I	100.03	27.20 (3.24)	108.43	–6.37 (1.53)
		II	119.20	2.13 (1.59)	111.87	28.97 (6.82)		111.87			
					120.63		II			122.93	8.93 (1.29)
										126.63	
	40 U HPA/	FL	53.03	1.03 (0.21)	53.48	4.27 (0.67)	FL				
	100 U HPA[a]	I	95.27	31.07 (1.20)	–	–	I	n.d.		n.d.	
		II	117.97	0.83 (0.51)	111.77	27.60 (3.27)	II				
					119.55						
	Acid	FL	–	–	–	–	FL				
		I	96.97	30.30 (1.77)	–	–	I	n.d.		n.d.	
		II	118.90	0.45 (0.07)	110.57	15.10 (5.11)	II				
DP950	*20 U HPA*	FL	51.93	1.87 (0.47)	51.85	1.87 (0.32)	FL	–	–	75.45	1.93 (0.55)
		I	96.07	20.97 (2.32)	–	–	I	100.10	24.37 (1.17)	101.53	17.43 (2.35)
		II	–	–	111.47	25.83 (0.42)	II	–	–	119.37	9.67 (0.06)
					119.30						

Abbreviations. FL, free lipid; I, type I complex; II, type II complex; n.d., not determined;'–', not observed. Standard deviation enthalpy between brackets.
[a] DP400-GMS-60 °C and DP400-GMS-90 °C complexes were hydrolysed with 40 and 100 U HPA, respectively.

both types I and II are present) increases with increasing amylose DP (DP60, DP400) but is again lower for the DP950-complexes.

Comparison of the thermal properties of amylose-lipid complexes before (Gelders et al., 2004) and after hydrolysis reveals that some lipid was released during hydrolysis. This happened to a larger extent for the shorter amylose DPs as $\Delta H_{\text{Freelipid}}$ augmented from practically zero to a maximum value of 8.7 J/g. Since, for the DP60-complexes the highest DH values (~40 and ~55%) were obtained, it is likely that more lipids are released from these structures. T_m was lower for complex residues than for the original complexes and decreased gradually when higher dosages of HPA or acid hydrolysis were applied. Compared to $\Delta H_{\text{complex}}$, $\Delta H_{\text{residue}}$ remained constant or increased somewhat after hydrolysis. For higher HPA dosages and acid hydrolysis of DP400-GMS-complexes, $\Delta H_{\text{residue}}$ is smaller than $\Delta H_{\text{complex}}$ as has been described in literature. Seneviratne and Biliaderis (1991) indeed reported a progressive reduction in ΔH and T_m when enzymic hydrolysis of types I, II_a or II_b amylose-GMS complexes proceeded. They also stated that enzymic treatment did not impact the crystallinity of the residues. These authors hypothesised that the presence of helical amylose chains that have little long range order (crystallinity) may be an important factor to $\Delta H_{\text{complex}}$. Assuming that these chains are more enzyme susceptible than well-developed crystallites, enzyme hydrolysis of the complexes will yield resistant residues with reduced ΔH and little change in their crystalline domains. Upon removal of the interconnecting amorphous chain segments between crystalline regions of the complexes, the latter show reduced thermal stability (i.e. lower T_m) than their native structures (Seneviratne & Biliaderis, 1991).

We believe that, in the early stages of hydrolysis when only interconnecting and amorphous amylose and few crystallites are hydrolysed, concentration of crystallites explains the increases in ΔH and relative crystallinity values. Moreover, hydrolysis of the interconnecting amorphous amylose chains increases the mobility of the whole structure, resulting in a reduced T_m. It is not until a certain level of crystallites has been hydrolysed, that ΔH and relative crystallinity decrease, as is the case for higher dosages of HPA and acid hydrolysis.

3.4. Molecular weight distribution of hydrolysis residues

Fig. 2 shows HPAEC-PAD profiles of DP60 [profile (iii)], DP60-GMS-60 °C [profile (iv)] and DP60-C22-60 °C [profile (v)]. HPAEC-PAD reveals very clearly that, by complexation with GMS, a dextrin population with DP> 30–35 is lifted from the DP60 fraction, and that, for complexation with C22, a minimum dextrin chain length of

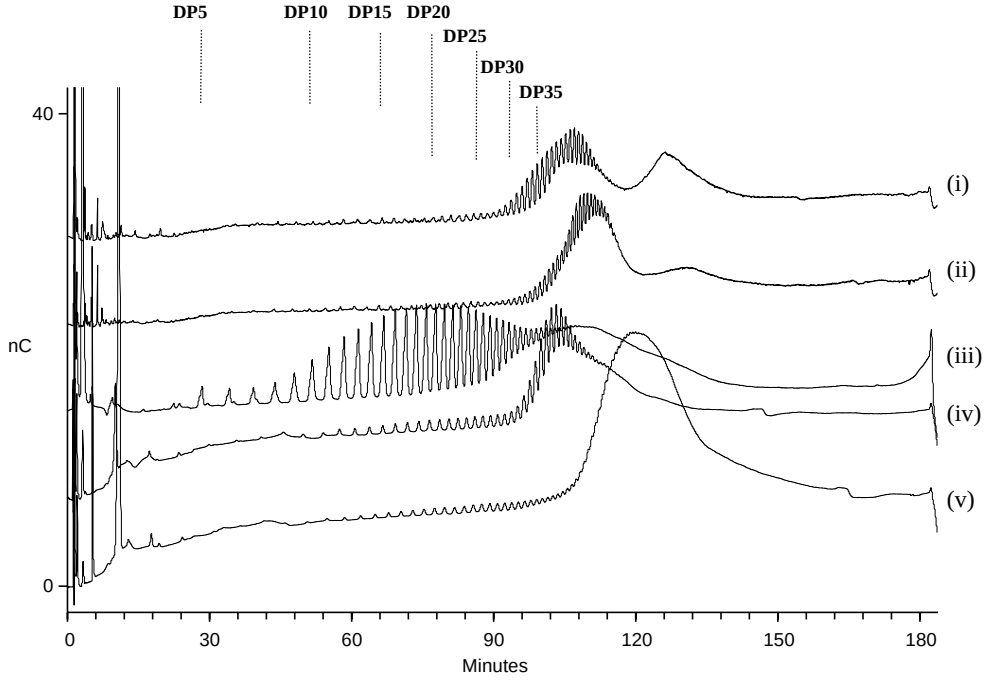

Fig. 2. High-performance anion-exchange chromatography with pulsed amperometric detection (HPAEC–PAD) profiles of (i) DP60-GMS-60 °C 20 U HPA residue; (ii) DP60-C22-60 °C 20 U HPA residue; (iii) DP60; (iv) DP60-GMS-60 °C and (v) DP60-C22-60 °C.

Table 4
Peak DP of different dextrin subpopulations obtained after enzymic (hog pancreatic alpha-amylase; HPA) or acid (2.2 N HCl) hydrolysis of complexes formed between amylose DP60, 400 and 950, and glyceryl monostearate (GMS) or docosanoic acid (C22) at 60 or 90 °C. Peak DP was calculated by means of a pullulan calibration curve specific for Superose 12TM column. Values between brackets is the dextrin length expressed in 'nm', assuming a V_6 helix with a pitch of 0.805 nm

Amylose	Hydrolysis	GMS		C22	
		60 °C	90 °C	60 °C	90 °C
DP60	20 U HPA	44 (5.9)	43 (5.8)	51 (6.8)	48 (6.4)
		95 (12.7)	99 (13.3)	113 (15.2)	104 (14.0)
					322 (43.2)
DP400	20 U HPA	46 (6.2)	79 (10.6)	55 (7.4)	56 (7.5)
		102 (13.7)	194 (26.0)	124 (16.6)	139 (18.6)
		189 (25.4)	311 (41.7)	204 (27.4)	214 (28.7)
	40 U HPA/100 U HPA[a]	46 (6.2)	71 (9.5)	–	–
		106 (14.2)	183 (24.6)	–	–
		189 (25.4)	283 (38.0)	–	–
	Acid	52 (7.0)	72 (9.7)	–	–
		102 (13.7)	167 (22.4)	–	–
DP950	20 U HPA	49 (6.6)	79 (10.6)	54 (7.3)	59 (7.9)
		110 (14.8)	209 (28.0)	130 (17.4)	137 (18.4)
		199 (26.7)	319 (42.8)	227 (30.5)	263 (35.3)

[a] DP400-GMS-60 °C and DP400-GMS-90 °C complexes were hydrolysed with 40 and 100 U HPA, respectively.

DP40 is required (Gelders et al., 2004). The respective 90 °C-complexes resulted in similar observations (not shown). These minimum chain lengths correspond to the length needed to accommodate two GMS- or C22-molecules within an amylose helix (Gelders et al., 2004). Hydrolysis with 20 U HPA produced two dextrin subpopulations with peak DP 43 and 95 for the DP60-GMS-60 °C complex residue [profile (i)] and peak DP shifted towards 50 and 113 for the DP60-C22-60 °C complex residue [profile (ii)] (see also Table 4). Other complex residues resulted in two or even more dextrin subpopulations as well when analysed with HPAEC-PAD (results not shown) or with HPSEC (Fig. 3).

These subpopulations are clearly distinguished for the first time. The peak DP of the successive fractions corresponds to '*n*' times that of the smallest peak DP plus some glucose moieties, presumably corresponding to the amorphous links between the lamellae (Table 4). The smallest peak DP, resembling the lamellar « unit » of the amylose-lipid complex, is about 44 (5.9 nm) for GMS-complexes and about 50 (6.7 nm) for C22-complexes and increases slightly with increasing amylose DP for the 60 °C-complexes. In other papers, DPs > 45 have indeed been mentioned for such residues as were lamellar thicknesses ranging between 7 and 20 nm (Biliaderis & Galloway, 1989; Galloway et al., 1989; Jane & Robyt, 1984). For complexes formed at 90 °C, peak DP increases significantly from 43 to 79 (GMS-complexes) and from 48 to 59 (C22-complexes) with increasing amylose DP. Crystal thickness (1.6–4.6 nm, determined with transmission electron microscopy) increases with amylose chain length (DP30, 40, 80, 900) for complexes formed at 90 °C as described by Godet et al. (1996). This is explained by the fact that the global level of organisation and crystal thickness is related to the crystallisation ability of amylose chains (determined by chain length) and the stabilising effect of the fatty acid molecules (depending on lipid length) (Godet et al., 1996). While the difference in DP of residual dextrins between 60 and 90 °C form is negligible for the DP60-complexes, it increases with increasing amylose DP, although less explicit for the C22-complexes. Galloway et al. (1989) stated—based on different melting temperatures for type I and II complexes—that complexes grown at 90 °C have thicker lamellae than the 60 °C complexes because of supercooling effects.

More severe hydrolysis of DP400-GMS-60 °C and DP400-GMS-90 °C complexes decreased the level of the highest DP subpopulations and enriched the smallest peak DP subpopulation or lamellar unit. However, the peak DPs remained constant. This is in agreement with Jane and Robyt (1984) who reported that hydrolysis beyond that needed to cleave the folding points, decreases the yield of resistant fragments but not their size. They therefore, concluded that hydrolysis of retrograded amylose, V_6, V_7 and V_8 amylose-alcohol complexes with different alpha-amylases (and different substrate binding domains) leads to amylodextrins with different average chain lengths and relatively narrow, molecular weight distribution. By varying amylose DP, lipid type and chain length, and complexation temperature of amylose-lipid complexes, the DP of residual dextrins obtained after hydrolysis can be influenced as well, as evidenced in this paper.

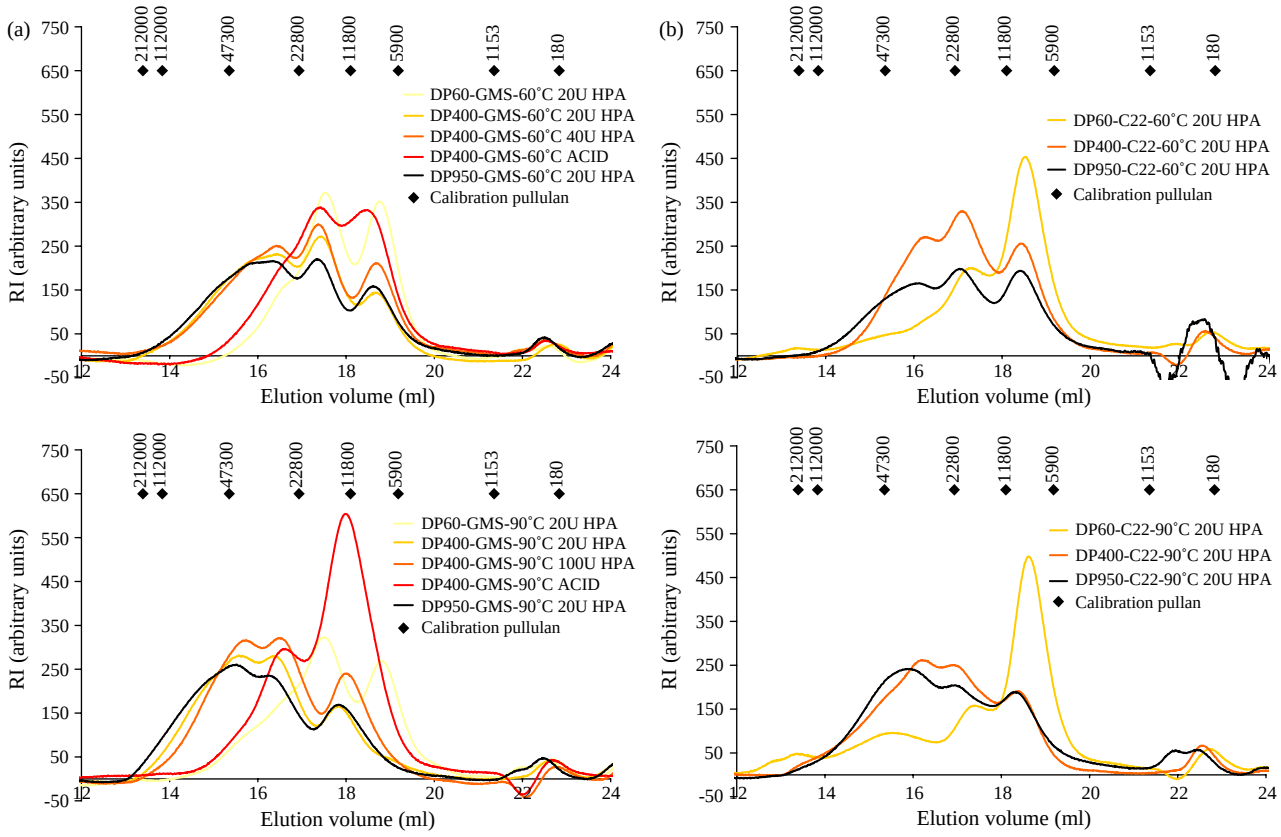

Fig. 3. Superose 12TM size-exclusion chromatograms of (a) GMS-complexes formed at 60 °C (upper) and 90 °C (lower) hydrolysed with 20, 40 or 100 U HPA or 2.2 N HCl, and of (b) C22-complexes formed at 60 °C (upper) and 90 °C (lower) hydrolysed with 20 U HPA.

4. Conclusions

Hydrolysis of DP60 amylose-lipid complexes, formed at either 60 or 90 °C, resulted in the highest DH and overlapping hydrolysis curves because a DP exceeding 60 is required to form type I and II complexes. DP400- and DP950-complexes were of type I or II when formed at 60 or 90 °C, respectively. This was reflected in a lower enzyme and presumably also acid resistance for the type I complexes. The longest amylose fractions and lipids, complexed at 90 °C, yielded the most resistant complexes. Hydrolysis yielded two or more dextrin subpopulations, interpreted as a sequence of lamellar « units » with interconnecting, amorphous amylose chains. As hydrolysis proceeds or higher dosages are applied, more and more helix interconnecting amylose chains are hydrolysed, resulting in enrichment of the lowest peak DP subpopulation. It is important to mention that the DP of these lowest peak DP subpopulations remains constant. By changing the amylose DP, lipid type and chain length, and complexation temperature (for the higher amylose DPs) of amylose-lipid complexes, dextrin subpopulations can be obtained—after enzymic or acid hydrolysis—with a relatively, narrow molecular weight distribution.

Acknowledgements

Amylum Europe N.V. (Aalst, Belgium), in particular Dr A. Vidts, is gratefully acknowledged for partial funding of this work. Prof. H. Reynaers and Dr B. Goderis (Laboratory of Macromolecular Structural Chemistry, K.U. Leuven, Leuven, Belgium) are thanked for access to X-ray infrastructure and technical assistance. Ir. R. Vermeylen is thanked for the fruitful discussion concerning this manuscript. We thank the Fund for Scientific Research-Flanders (Fonds voor Wetenschappelijk Onderzoek-Vlaanderen) for financing the Research Assistantship of G. G. Gelders.

References

Biliaderis, C. G., & Galloway, G. (1989). Crystallization behavior of amylose-V complexes: structure-property relationships. *Carbohydrate Research*, *189*, 31–48.

Biliaderis, C. G., & Seneviratne, H. D. (1990). On the supermolecular structure and metastability of glycerol monostearate-amylose complex. *Carbohydrate Polymers*, *13*, 185–206.

Buléon, A., Colonna, P., Planchot, V., & Ball, S. (1998). Mini review. Starch granules: Structure and biosynthesis. *International Journal of Biological Macromolecules*, *23*, 85–112.

de Claubry, G. (1814). *Gilbert's Annals of Physics* (Adapted from 'Starch and its derivatives; volume one' J.A. Radley (1953). Ed. Chapmann and Hall Ltd, London, UK, 510p)..

Dubois, M., Gilles, K. A., Hamilton, J. K., Rebers, P. A., & Smith, F. (1956). Colorimetric method for determination of sugars and related substances. *Analytical Chemistry*, *28*(3), 350–356.

Eliasson, A.-C., & Krog, N. (1985). Physical properties of amylose-monoglyceride complexes. *Journal of Cereal Science*, *3*, 239–248.

Englyst, H. N., & Cummings, J. H. (1984). Simplified method for the measurement of total non-starch polysaccharides by gas-liquid chromatography of constituent sugars as alditol acetates. *Analyst*, *109*, 937–942.

Galloway, G. I., Biliaderis, C. G., & Stanley, D. W. (1989). Properties and structure of amylose-glyceryl monostearate complexes formed in solution or on extrusion of wheat flour. *Journal of Food Science*, *54*(4), 950–957.

Gelders, G. G., Bijnens, L., Loosveld, A.-M., Vidts, A., & Delcour, J. A. (2003). Fractionation of starch hydrolysates into dextrins with narrow molecular weight distribution and their detection by high-performance anion-exchange chromatography with pulsed amperometric detection. *Journal of Chromatography A*, *992*, 75–83.

Gelders, G. G., Vanderstukken, T. C., Goesaert, H., & Delcour, J. A. (2004). Amylose-lipid complexation: a new fractionation method. *Carbohydrate Polymers*, *56*, 447–458.

Godet, M. C., Bizot, H., & Buléon, A. (1995). Crystallization of amylose-fatty acid complexes prepared with different amylose chain lengths. *Carbohydrate Polymers*, *27*, 47–52.

Godet, M. C., Bouchet, B., Colonna, P., Gallant, D. J., & Buléon, A. (1996). Crystalline amylose-fatty acid complexes: morphology and crystal thickness. *Journal of Food Science*, *61*(6), 1196–1201.

Godet, M. C., Tran, V., Colonna, P., Buléon, A., & Pezolet, M. (1995). Inclusion/exclusion of fatty acids in amylose complexes as a function of the fatty acid chain length. *International Journal of Biological Macromolecules*, *17*, 405–408.

Holm, J., Björck, I., Ostrowska, S., Eliasson, A.-C., Asp, N.-G., Lundquist, I., & Larsson, K. (1983). Digestibility of amylose-lipid complexes in-vitro and in-vivo. *Starch/Stärke*, *35*(9), 294–297.

Jane, J.-L., & Robyt, J. F. (1984). Structure studies of amylose-V complexes and retrograded amylose by action of alpha amylases, and a new method for preparing amylodextrins. *Carbohydrate Research*, *132*, 105–118.

Kitahara, K., Suganuma, T., & Nagahama, T. (1996). Susceptibility of amylose-lipid complexes to hydrolysis by glucoamylase from *Rhizopus niveus*. *Cereal Chemistry*, *73*, 428–432.

Kowblansky, M. (1985). Calorimetric investigation of inclusion complexes of amylose with long-chain aliphatic compounds containing different functional groups. *Macromolecules*, *18*, 1776–1779.

Robin, J. P., Mercier, C., Charbonnière, R., & Guilbot, A. (1974). Lintnerized starches. Gel filtration and enzymatic studies of insoluble residues from prolonged acid treatment of potato starch. *Cereal Chemistry*, *51*, 389–406.

Robin, J. P., Mercier, C., Duprat, F., Charbonnière, R., & Guilbot, A. (1975). Amidons lintnérisés. Etudes chromatographique et enzymatique des résidus insolubles provenant de l'hydrolyse chlorhydrique d'amidons de céréales, en particulier de maïs cireux. *Starch/Stärke*, *27*(2), 36–45.

Roger, P., Axelos, M. A. V., & Colonna, P. (2000). SEC-MALLS and SANS studies applied to solution behavior of linear alpha-glucans. *Macromolecules*, *33*, 2446–2455.

Seneviratne, H. D., & Biliaderis, C. G. (1991). Action of alpha-amylases on amylose-lipid complex superstructures. *Journal of Cereal Science*, *13*, 129–143.